WM 4:00 PM - 5:30 PM

B313B-B314

Optical MEMS Components

Joseph Ford, *OMM, USA, Presider*

WM1 **4:00 PM**

Nonlinear Servo Control of MEMS Mirrors and Their Performance in a Large Port-Count Optical Switch

I. Brener, P. Chu, M. Tsai, C. Pu, M. Chou, J. Dadap, D. Lee, B. Tang, D. Peale, N. Bonadeo, R. Harel, C. Wu, J. Johnson, S. Park, S. Lee, D. Tong, R. Doran, K. Bergman, T. Chau, E. Goldstein, L. Lin, J. Walker, W. Zhong, R. Gibson, *Tellium, Oceanport, NJ, Email: igal@comcast.net.*

We demonstrate full closed-loop control of electrostatically actuated double-gimbaled MEMS mirrors and use them in a free space optical cross-connect with switching times of less than 10ms, and optical power stability of better than 0.2 dB.

1. Introduction

In high port count 3D-MEMS optical crossconnects (OXC) [1] one is typically faced with the challenge of achieving as large a mirror angular swing as possible with a minimum separation between the ports to achieve low optical loss. MEMS based OXCs demonstrated to date use open loop architecture. The physics of an electrostatically actuated MEMS gimbal mirror dictates that the mirror becomes unstable at a certain angle commonly referred to as the "snap-down" angle [2], which lies between 1/3 and 1/2 of the mirror "touchdown" angle (i.e., when the mirror plate physically contacts the underlying electrodes). Thus, under open loop control, the rule of thumb is to limit the mirror tilt angles to less than a third of the touchdown angle. Stated differently, the physical air gap employed is more than three times larger than necessary to achieve the physical swing angle desired resulting in unnecessarily high drive voltage requirements.

Additional complexity in OXC systems arises from the extremely high pointing accuracy required, regardless of the technology used. Typically, an angular misalignment of the order of 100 μrad is all it takes to increase the optical loss by fractions of a dB. Maintaining such a pointing accuracy of MEMS mirrors over long periods of time is a challenge, given the maturity of this technology. Also, stochastic perturbations such as shock and vibration can introduce mechanical misalignment into the mirror position leading to severe penalties in optical performance.

All of these issues can be eliminated through the use of active position control of the MEMS mirrors. Servo controlled mirrors can be actuated far beyond the snap-down angle [3] thereby reducing the air gap and thus drive voltage. Servo control also provides corrective action to eliminate position drift that occurs through either internal mechanisms such as charge build-up or external means such as vibration or shock.

2. MEMS mirror description and servo controller design

The MEMS mirrors used in this work are 2-axis gimbaled tilting mirrors made of 10μm thick single-crystal silicon with radiuses from 400 to 450μm. The mirrors are suspended by torsional springs, and are designed to have resonant frequencies at zero deflection angle between 300 and 400 Hz (both axes). The Q value in air for both axes is ~3-5. The mirror is actuated through the application of voltages to four electrodes located 80μm underneath the mirror with the geometry shown in Fig. 1(a). Every quadrant electrode can be further divided in an optimal fashion between driving and sensing electrode. The sensing

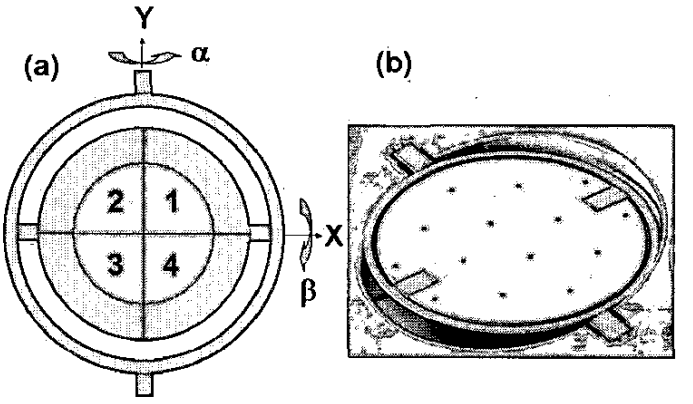

Fig. 1. (a) Schematic diagram of the double-gimbaled mirror used in this work (b) a micrograph of the actual MEMS mirror.

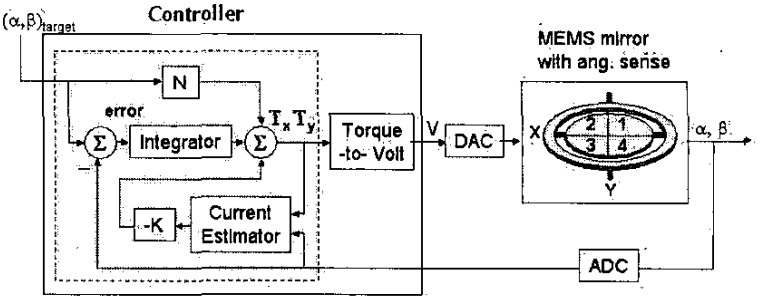

Fig. 2. Block diagram of the MEMS servo control harware and software.

portion can be used for angular sensing through differential capacitance measurements [4]. In this work, the MEMS mirror position is detected by optical means, however, capacitive and optical sensing methods are both compatible with our control approach.

In dealing with the electrodynamics of these types of structures, a number of simplifying assumptions have to be made. If their effect is small, then they can be bundled into the margin that a good servo design has to account for (this is not the case for an open loop system though). These assumptions are: i) we neglect any electrostatic action on the mirror springs; ii) we treat only torsional motion and neglect any other modes; iii) torsional springs have linear angle and torque relationship; iv) we neglect all inter-axis mechanical coupling (but not coupling in the electrostatic torque); v) the mirror damping is independent of angle.

Let's call α the angle around the gimbal axis (Y) and β the angle around the mirror axis (X). Then the equations of motion around both axes are given by:

$$J_Y\, d^2\alpha/dY^2 + \gamma_Y\, d\alpha/dY + K_Y\alpha = T_Y(\alpha,\beta)$$
$$J_X\, d^2\alpha/dX^2 + \gamma_X\, d\alpha/dX + K_X\alpha = T_X(\alpha,\beta) \qquad (1)$$

$T_{X,Y}(\alpha,\beta)$ are the electrostatic torques, $\gamma_{X(Y)}$ the damping parameters, $J_{X(Y)}$ the moments of inertia, and $K_{X(Y)}$ the torsional spring stiffness. $J_{X(Y)}$ can be estimated based on geometry, and $K_{X(Y)}$ and $\gamma_{X(Y)}$ can be determined experimentally.

Equations (1) describe a classical two-dimensional second order linear system, for which well-known linear control techniques can be used to design a controller using torque as the control variable [5]. The torques $T_{X,Y}(\alpha,\beta, V_1, V_2, V_3, V_4)$, depend in a nonlinear fashion on the two angles and four electrode voltages, which are the actual control inputs to the electrostatic system. If one can establish a good knowledge of this nonlinearity, the necessary applied voltages can then be determined using an inverse torque function.

We can approximate the electrostatic torques based on mirror symmetry with the following formulas:

$$T_X(\alpha,\beta) = f(\alpha,\beta)\, V_4^2 + f(-\alpha,\beta)\, V_3^2 - f(-\alpha,-\beta)\, V_2^2 - f(\alpha,-\beta)\, V_1^2$$

$$T_Y(\alpha,\beta) = g(\alpha,\beta)\, V_4^2 - g(-\alpha,\beta)\, V_3^2 - g(-\alpha,-\beta)\, V_2^2 + g(\alpha,-\beta)\, V_1^2 \qquad (2)$$

where $f(\alpha,\beta) = 1/2\ dC(\alpha,\beta)/d\hat{a}$ and $g(\alpha,\beta) = 1/2\ dC(\alpha,\beta)/d\alpha$.

$C(\alpha,\beta)$ is the driving electrode capacitance with respect to the mirror node (it is assumed to be the same for all quadrants).

Under servo operation, the torques $T_{X,Y}(\alpha,\beta)$ are calculated by the controller. Then one needs to find a combination of voltages that will provide these torques. Eq. (2) represents two equations with four variables to solve ($V_{1..4}$), and thus the system is overdetermined. One possible solution to eq. (2) is to require that at any given time, at most two voltages are non-zero. This solution reduces the number of analog to digital converters (ADCs) that are required to drive each mirror from four to just two, but adds analog switches.

This approach shifts most of the complexity of the servo design to the torque inversion problem. There is no simple way of measuring the capacitances $C(\alpha,\beta)$, and thus some modeling simplifications have to be made. We can treat the functions $f(\alpha,\beta)$ and $g(\alpha,\beta)$ as empirical tables, and by measuring the equilibrium voltages and angles for a given discrete grid, we can populate their values. However, for this procedure to be effective the mirror needs to be driven beyond snapdown angles, which can only be done under servo control. Therefore, a first estimate of the capacitance $C(\alpha,\beta)$ is done using numerical methods. This initial torque guess is usually sufficient to servo the mirror to some angle past snapdown.

The main performance parameters required from the servo-controlled mirror are i) switching time<10 ms (mirror angle within 150 μrad of target angle), ii) maximum angular deviation due to noise less than 75 μrad per axis, iii) noise

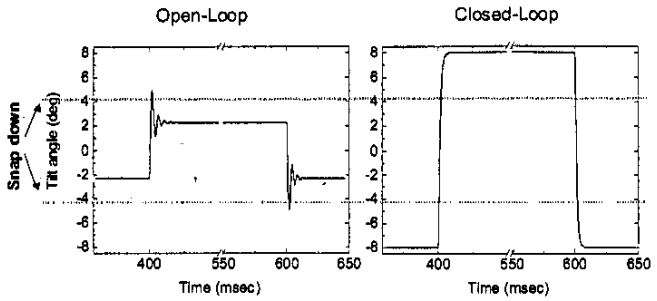

Fig. 3. Comparison of switching under open loop and closed loop operation. The closed loop angular trajectory can exceed the snapdown angle and shows no overshoot.

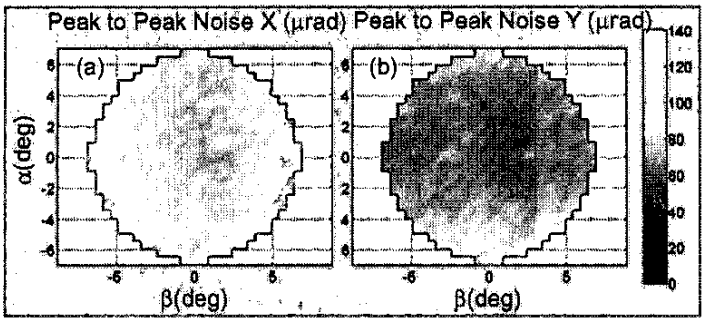

Fig. 4. A colormap representation of the peak to peak noise under servo operation and for both axis.

rejection and vibration immunity, iv) a finite available control voltage of less than 85V.

We use state space techniques to design a digital controller with full-state feedback. A current estimator is used to estimate the angular position and velocity of each mirror axis. In addition, we include an integrator and a feedforward term to compensate for the extra pole introduced by the integrator [5]. We choose the controller poles at 200Hz with estimator and integrator poles 4 to 6 times faster, and a damping ratio of 1, which provides no angular overshoot. A schematic representation of the controller design is shown in Fig. 2.

3. Performance and optical switching under servo control

The servo control coding was implemented using a 100MHz 600FLOPS (32-bit floating point) digital signal processor (ADSP-21161N) with interfaces to multiple ADC and DACs (16/12 bit resolution). After code optimization, a single DSP could servo 8 mirrors with a sampling rate of 20KHz (or 16 mirrors at 10KHz).

A comparison between open and closed loop switching is shown in Fig. 3 for single axis switching. It is obvious from this figure that the servo controller removes the angular limitation imposed by the instability past snapdown. The touchdown angle for this axis is 10.3 degrees, and thus we were able to servo successfully up to 75% of the angular range. The maximum angle that can be achieved with such controller is limited by the reduction of phase margin caused by the finite sampling time combined with the mirror moving in the unstable regime. Other factors, such as modeling imperfections, neglected resonances, etc. can contribute too. Despite the short switching time, the maximum voltage under servo operation never exceeds 85V.

The most stringent measure of success is the steady state angular noise. In order to quantify this, we record the peak angular noise around the target angle over a period of several minutes, and for a full mesh of angles spanning +-7 degrees for both axes. This noise was recorded using the same angular sense circuitry used for servo control, and thus had an additional 25-50 μrad noise coming from this circuitry alone.

The peak-to-peak noise map is shown in Fig. 4. The optical power stability requirement (<0.5dB) mandates that the angle stability for a single mirror has to be better than 150 μrad around the target angle. This corresponds to a maximum of 300 μrad peak-to-peak noise requirement, a number easily met by this controller and plant.

Finally, we use two of these closed-loop controlled mirrors in a free-space modular optical switch. The distance between the mirrors is ~2m and the beam diameter is ~2mm. Fig. 5(a) shows a switching event commanded to one mirror. The switching time, as determined from the fiber-coupled optical power is of the order of 5ms, and it was fairly independent of the angular swing (this is expected in a closed-loop design). When both mirrors are under closed loop control and establishing a connection, the fluctuations in the optical power are of the order of 0.1-0.2 dB, very close to the target values. This is shown in Fig. 5(b).

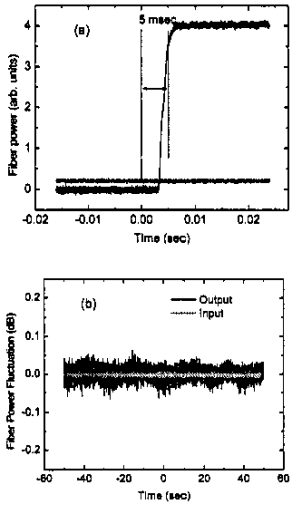

Fig. 5. (a) a single-mirror switching event as observed through the fiber-coupled optical power when two parts establish a connection. (b) optical power stability under a stable connection. The angles used for these measurements were close to 5 degrees, which is beyond snapdown.

In conclusion, we demonstrate full closed-loop control of electrostatically actuated MEMS mirrors and their performance in a free space optical crossconnect. The mirrors can be driven well beyond their snapdown angle with long term angular noise of less than 150 μrad. We use these closed loop controlled mirrors in a free space optical crossconnect, and achieve switching times <10ms and optical stability of better than 0.2dB.

References

[1] P.B. Chu *et al*, *IEEE Communication Magazine*, (80) March 2002.
[2] O. Degani, et al., *JMEMS*, 7(4), 373 (1998).
[3] M.S.C. Lu and G.K. Fedder, *Tech. Dig. IEEE Solid-State Sensor Actuator Workshop*, Hilton Head Island, 255 (2002).
[4] S. Blackstone and T.J. Brosnihan, *Proc. IEEE/LEOS Int. Conf. Optical MEMS'01*, Okinawa, Japan, 35 (2001).
[5] G.F. Franklin *et al.*, *Digital Control of Dynamic Systems*, Addison Wesley, Menlo Park, California, 1998, pp.323-325.

WM2 **4:15 PM**

Insertion Loss Model and Input/Output Losses of Single-Stage Optical Cross-Connects

R. Capik, J. Hickey, S. Korotky,
Lucent Technologies, Holmdel, NJ,
Email: skk@lucent.com.

We propose and demonstrate an effective model of the insertion loss of single-stage optical cross-connects, which has application to improve the speed and quality of connection training, to reduce the size of the loss table, and to facilitate maintenance.

1. Introduction

Only a very few optical switching technologies are capable of achieving input/output port counts in the range of 1000×1000 and beyond.[1] Among the options, switch fabrics based on free-space optical beam-steering have proven practical and have been brought to market. These switches not only provide high port count, but also achieve low insertion loss, high connection-to-connection isolation, fast reconfiguration speed, and offer the very high degree of bit-rate and format independence that is characteristic of passive optics.[2-5]

Beam-steering switches permit connections between very large numbers of ports within a single stage because each of the individual inputs and outputs may be set to a large number of states, namely the angles to which the beam is steered. The tradeoff for the relative ease of achieving large port counts using beam-steering is the increase in complexity of controlling the steering mechanisms. To aid in training, targeting and verifying connections, it can be useful to measure the insertion loss attained for a connection and compare it to a reference (eg. minimum) insertion loss for that connection. As the number of connections grows quadratically with the number of I/O ports, n, training and verifying all connections of a large port count switch can be challenging and time-consuming. Storing the insertion loss values for all n^2 possible connections in the onboard memory of controllers may also be inconvenient and costly when n is very large.

Here we introduce an effective model for the insertion loss of single-stage, beam-steering optical switches and cross-connect network elements that reduces the number of independent variables describing the n^2 insertion losses by a factor of $n/2$. Consequently, the model may be applied to reduce the size of the table representing the insertion losses. Most important, it serves as a powerful tool to speed and increase the quality, or accuracy, of the connection training.

2. Loss Model

We consider a single-stage optical switch that has n input ports and n output ports. As there is a unique path from every input (I) to every output (O) for a single-stage switch, there are a total of n^2 I/O paths. Each path has an associated optical insertion loss, which we denote as I_{ij}. Here, i identifies the input port and j identifies the output port. Consequently,